A Two-Dimensional Satellite Rainfall Error Model

Faisal Hossain and Emmanouil N. Anagnostou

***Abstract*—A two-dimensional satellite rainfall error model (*SREM2D*) is developed for simulating ensembles of satellite rain fields on the basis of "reference" rain fields derived from higher accuracy sensor estimates. With this model we aim at characterizing the multidimensional stochastic error structure of satellite rainfall estimates as a function of scale. The pertinent error dimensions we seek to address are: 1) the joint probability density function for characterizing the spatial structure of the successful delineation of rainy and nonrainy areas; 2) the temporal dynamics of rain estimation bias; and 3) the spatial variability of rain rate estimation error. Ground radar rain fields in the Southern plains of the United States are used as reference to evaluate *SREM2D* error parameters at 0.25-deg and hourly spatiotemporal resolution for an infrared (IR) rain retrieval algorithm (IR-3B41RT) developed at NASA. Comparison of *SREM2D* simulated satellite rainfall with actual IR-3B41RT data showed that the error modeling technique can preserve the estimation error characteristics across scales with marginal deviations. The model performance is compared against two simpler, but widely used, approaches of error modeling that do not account for uncertainty in rainy/nonrainy area delineation. It is shown that both of these approaches fare poorly with regards to preserving the error structure across scales. They underestimated the sensor retrieval error standard deviation by more than 100% upon aggregation, which, for *SREM2D*, was found to be below 30%. *SREM2D* is modular in design—it can be applied for any satellite rainfall algorithm to consistently characterize its error structure.**

***Index Terms*—Error model, error propagation, infrared (IR), satellite rainfall estimation, scale.**

I. Introduction

OUR ability to accurately model the error structure of satellite rainfall at fine space-time scales (<0.1 deg, and 1- to 3-hourly) is currently of high importance due to the anticipated increased availability of passive microwave (PM) satellite sensor observations from the Global Precipitation Measurement mission (GPM) [5]. GPM observations combined with high-frequency rainfall estimates available from geostationary infrared (IR) sensors [20] as well as auxiliary data (such as long-range lightning observations [7], [39]) and multisensor estimation techniques [24], [28], [18]) are expected to yield global rainfall products of improved accuracy, and consequentially expanded levels of utility. In this respect, an adequately designed satellite rainfall error model capable of generating realistic ensembles of high resolution satellite rain fields from reference rain fields of higher accuracy (e.g., dense surface gauge network or ground radar) is mandated. Developing probabilistic (ensemble) representations of the error propagation from satellite rainfall products to high-resolution hydrologic model simulations can form the basis for the establishment of criteria for the optimal use of satellite rainfall data in hydrologic forecasting and continental water and energy cycle studies [15], [16].

Two specific applications of satellite-rainfall error propagation need special reference in this context: 1) the Global Land Data Assimilation—*GLDAS* [32] and 2) the streamflow (or flood) prediction over ungauged regions [14], [15], [17], [29]. One of the primary objectives of *GLDAS* is to provide real-time and high resolution estimates of the surface hydrologic state that is of vital importance for the accurate forecasting of weather patterns [7]. The effectiveness of *GLDAS* depends largely on the quantification of the error structure of the hydro-meteorological forcing variables, which dictates the frequency for assimilation of satellite data [38]. Among the major hydro-meteorological forcing variables, rainfall is undoubtedly the most important component of the terrestrial water cycle. A recent study by Syed *et al.* [35] has shown that almost 70%–80% of the variability of the land surface hydrology is attributable to rainfall. On the other hand, a substantial portion of floods takes place in regions that are remote, or lack the financial resources to be adequately covered by ground stations [14]. A situation that further aggravates the global flood prediction problem is that several countries have most (more than 95%) of their territory within one or more international river basins [12], thus forced to cope with flooding primarily generated beyond their borders (e.g., the Bangladesh delta in the Ganges, Brahmaputra, and Meghna river basins [30]). The vantage of meteorological satellites provides a way of monitoring rainfall across political boundaries or ungauged terrain, which appears a plausible alternative for enhancing the flood forecasting capability of many flood prone lowermost riparian nations. It is the hydrologic time lag (between rainfall and the occurrence of flood peak downstream, which magnifies as a function of basin size) that comprises the fundamental principle for anticipating extension of forecasting range with quasi real-time satellite rainfall data. However, the accuracy in predicting sensitive flood parameters such as peak runoff and time-to-peak is dependent on our ability to monitor the spatiotemporal variability of rainfall. Although satellite observations provide the means for estimating rainfall over large-scale watersheds their estimates are associated with error. Proper characterization of the error and its nonlinear propagation in hydrologic models is, therefore, a critical priority that needs to be resolved.

For the accurate modeling of satellite rainfall error, it is important to recognize that the desired progression to finer

Manuscript received February 2, 2005; revised May 20, 2005. This work was supported in part by NASA's Global Water and Energy Cycle under Program NAG5-11527.

F. Hossain is with the Department of Civil and Environmental Engineering, Tennessee Technological University, Cookeville, TN 38505-0001 USA.

E. N. Anagnostou is with Department of Civil and Environmental Engineering, University of Connecticut, Storrs, CT 06269 USA (e-mail: manos@engr.uconn.edu).

Digital Object Identifier 10.1109/TGRS.2005.863866

space-time scales in satellite rain estimation is counter-balanced by an increasing multidimensionality of the retrieval error. This scale dependence of rain retrieval error is associated with complex error propagation in hydrologic modeling through the highly nonlinear and fast-evolving land-atmosphere processes [3], [15], [16]. As an example, consider the case of vertical soil moisture transport. The water flux in soil is governed by the cumulative effect of infiltration, runoff, gradient diffusion, gravity, and soil water extraction through roots for canopy transpiration. All these processes exhibit dynamic variability in the ranges of minutes to hours over scales of squared centimeters to squared kilometers. Hence, a land surface model (LSM) requires the numerical solution of a second-order partial differential equation at fine step-lengths to adequately capture the spatiotemporal variability of the soil water movement (for a list of equations typically used by LSMs, see Dai *et al.*, [8]). On the other hand, past satellite rainfall studies have concentrated on rain retrieval uncertainty issues associated with large spatiotemporal scales involving limited number of error statistics [13], [1], [28]. These statistics are useful mainly in assessing the use of satellite rainfall data in long-term climatologic or water balance studies, but they cannot offer any insight toward gauging the more dynamic and finer scale phenomena such as, for example, soil water movement, floods and weather-related hazards.

In addition to the scale issue, current satellite error models target mostly PM sensor retrievals focusing primarily on the sampling uncertainty due to the low frequency of satellite overpasses (for a detailed review see [2]; Steiner *et al.* 1996; Bell, 1987; Bell *et al.*, 1990, [36], and [10]). To the best of our knowledge, there currently exists no modeling technique that mathematically accounts for uncertainty in delineation of rainy and nonrainy areas by satellite sensor observations. Recently, Hossain and Anagnostou [15], [16] have provided evidence that a detailed decomposition of the satellite rainfall error structure with explicit formalization of the uncertainty in rainy/nonrainy area delineation can contribute to improving our understanding of the implications of satellite estimation error on land surface simulation parameters for fine-scale hydrological processes (such as floods and soil moisture dynamics). However, recent error propagation studies continue to lack explicit acknowledgment of these unavoidable components of the fine-scale error structure (see, for example, [29] and [38]).

The herein study, motivated by the current state of the art in error modeling and the challenges we are faced by the need for high-resolution satellite rainfall data, mathematically formalizes a space-time error model, named a two-dimensional satellite rainfall error Model (*SREM2D)*. Because the accuracy in satellite-based land surface hydrologic simulation depends on an accurate characterization of the rainfall estimation error our goal is to provide an objective framework for error propagation studies. *SREM2D* is conceptualized based on the following design objectives: 1) It should function as a filter wherein the hydrological implications of fine-scale components of the satellite precipitation error structure can be explicitly determined by coupling it with a hydrological/LSM; Thus, *SREM2D*-based experiments should provide the much needed focus to meteorologists for the development of improved satellite rainfall products with enhanced societal applications. 2) It should be modular in design with the capability to allow uncertainty assessment of any satellite rainfall algorithm. 3) It should be conceptualized in an algorithmic fashion so that it is easy to code for a user wishing to make use of the model. *SREM2D* uses as input "reference" rain fields of higher accuracy and resolution representing the "true" surface rainfall process, and stochastic space-time formulations to characterize the multidimensional error structure of satellite retrieval. The algorithmic approach is aimed at generating realistic ensembles of satellite rain fields from the most definitive "reference" rain fields that would preserve the estimation error characteristics at various scales of aggregation. To demonstrate the relative accuracy of *SREM2D*, we also show comparisons with two commonly adopted satellite error modeling strategies in error propagation studies.

The paper is organized as follows. Section II presents the algorithmic formulation for *SREM2D*. Section III discusses calibration of the model parameters based on actual data. In Section IV, we evaluate the error model in terms of its numerical accuracy and scaling consistency, followed by a comparison with two simpler approaches. Finally, in Section V, we present our conclusions and future directions.

II. Formulation of the SREM2D Algorithm

SREM2D builds upon a one-dimensional version (point-versus-time) developed by Hossain and Anagnostou [15]. The original concept of the Hossain and Anagnostou [15] error model was to corrupt time series of point reference rainfall values to characterize the error structure of pertinent satellite estimates at sensor resolution. In this paper, we extend the concept in a method developed for simulating ensembles of satellite rain retrieval fields with coherent spatial error structures in terms of rain/no-rain detection and the estimation of rain rates in rain covered areas, and temporal variability in the marginal (mean and variance) rain rate error statistics. In the following, we describe the steps involved in the algorithm.

A. Step 1: Conversion of Time-Aggregated Reference Rain Rates to Represent Instantaneous Rain Rates

Ground based radar-rainfall or dense-gauge measurements, which are intended as "reference," are typically available at temporal scales coarser (>hourly) than the nearly instantaneous satellite retrievals. To address this issue an approach is devised to quantify the statistical departure of instantaneous from time-averaged rainfall rates at the satellite sensor resolution. We define two characteristics in this regard: 1) the difference in rain detection and 2) conditional rain rate differences (given successful detection at both aggregated and instantaneous scales). The "probability of detection" of instantaneous rain rate $(\mathrm{POD}_{\mathrm{INST}})$ is used to define the chance of an instantaneous reference measurement to register a nonzero value in agreement with the time-aggregated (hereafter, termed "accumulated") measurement. This is defined as follows:

$$\mathrm{POD}_{\mathrm{INST}} = \mathrm{Prob}\{R_{\mathrm{REF-INST}}>0 | R_{\mathrm{REF-ACCU}}>0\} \quad (1)$$

where $R_{\mathrm{REF-INST}}$ represents realizations of an instantaneous area-averaged reference rain rate value and $R_{\mathrm{REF-ACCU}}$ is the

accumulated reference rainfall of the corresponding time-step. The conditional error, $E_{\mathrm{INST-ACCU}}$, of $R_{\mathrm{REF-INST}}$ with respect to $R_{\mathrm{REF-ACCU}}$ is defined as

$$E_{\mathrm{INST-ACCU}} = R_{\mathrm{REF-INST}}/R_{\mathrm{REF-ACCU}}. \tag{2}$$

Due to the multiplicative nature of the error, the statistical distribution of $E_{\mathrm{INST-ACCU}}$ is assumed log-normal, with mean and variance components defined as $Mu_{\mathrm{INST-ACCU}}$ and $S_{\mathrm{INST-ACCU}}$, respectively. The above approach can be used to statistically generate instantaneous reference rain rates $(R_{\mathrm{REF-INST}})$ from, for example, hourly "reference" radar-rainfall values $(R_{\mathrm{REF-ACCU}})$. Hossain and Anagnostou [15] provide an example of the accumulated-to-instantaneous conversion on the basis of continuous record of gage rainfall data. This step can be ignored if reference rain fields are available at high temporal resolution (<1 h), or for example, they are themselves similarly instantaneous as the satellite rain fields (e.g., ground radar scans). From this conversion onwards, we shall continue to use the term reference rain fields to refer to instantaneous reference fields.

An instantaneous satellite rain retrieval (hereafter, we make no distinction between the words "retrieval" "estimation/estimate"), may exhibit one of the following possible outcomes: 1) when it actually rains (reference rainfall >0 unit) the satellite retrieval may indicate rain (successful rain detection) or zero rain (false no-rain detection), while 2) when it does not rain (reference rainfall = 0 unit) the satellite retrieval may indicate zero rain (successful no-rain detection) or nonzero rain (false rain detection—also termed as "false alarm"). We define the successful rain detection probability P_{RAIN} as a function of $R_{\mathrm{REF-INST}}$. The functional form is identified through calibration on the basis of actual data (discussed in the following section). The false no-rain detection is derived from P_{RAIN} as $(1-P_{\mathrm{RAIN}})$. The successful no-rain detection, P_{NORAIN}, is the unitary probability that satellite retrieval is zero when $R_{\mathrm{REF-INST}}$ is zero, which is also determined on the basis of actual data. The false rain detection probability is then derived from P_{NORAIN} as $(1-P_{\mathrm{NORAIN}})$. A probability density function (D_{false}) is defined to characterize the probability distribution of the satellite retrievals in false rain detection. This function is also identified through calibration on the basis of actual sensor data (discussed next in Section III). Note that the P_{RAIN} and P_{NORAIN} combined define the uncertainty of a satellite in delineation of rainy and nonrainy areas.

B. Step 2: Modeling the Joint Probability of Successful Delineation of Rainy and Nonrainy Areas

In this step, the joint spatial probability of successful delineation of rainy and nonrainy areas is characterized using Bernoulli trials of the uniform distribution with a correlated structure generated based on Gaussian random fields. These Gaussian random fields are transformed into uniform distribution random fields via an error function transformation. Modeling the spatial structures for detection is an important element of *SREM2D* as real sensor data are known to exhibit definitive spatial clusters for false rain and false no-rain detection. Fig. 1 shows an example of typical spatial structures expected

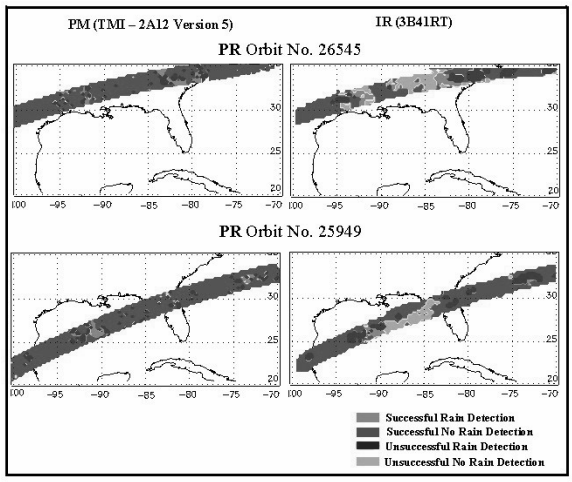

Fig. 1. Successful and unsuccessful rainy and nonrainy area delineation by PM (TMI) and IR (3B41RT) sensors referenced with TRMM-PR 2A25 rain observations. Left panels—TMI; Right panels—IR.

in the detection of rainy and nonrainy areas for PM and IR rainfall retrievals. In this figure, we use the more definitive tropical rainfall measuring mission (TRMM) precipitation radar (PR) rainfall fields [23] as reference. Ground validation studies on PR have shown high correlation (>0.9) and low (<7%) systematic differences with rain-gauge-calibrated ground radar estimates [4], [25]. The PM retrievals are represented by the 2A12 TRMM product computed with the Goddard profiling algorithm (GPROF) [24] (Fig. 1, left panels). In terms of IR retrievals, we used the hourly PM-calibrated variable IR rainfall product (VAR) produced by multisatellite precipitation analysis (MPA) [19] (Fig. 1, right panels). This product is operationally known as IR-3B41RT. On the common PR orbit, green and blue colors are used to identify successfully detected rainy and nonrainy pixels, respectively, while we use orange and red colors for the converse (unsuccessful detection). The spatial clusters of colors seem to indicate that sensor detection has a spatial dependency, which for IR retrievals appears to be more widespread and spatially correlated in the false detection situation (Fig. 1, right panels).

To model this spatial structure for detection, spatially correlated fields of Gaussian $N(0,1)$ random deviates are generated in 2-D space based on the Turning Bands algorithm [26]. A simple exponential type auto-covariance function is assumed. The correlation length (the separation distance at which correlation is equal to *et al.*, 0.3678) is determined on the basis of calibration with actual data over a large domain (the size of Oklahoma in this study). For identifying the correlation length of rainy (nonrainy) areas, we assign all successfully detected rainy (nonrainy) pixels the value of one while the rest are assigned zero values. Subsequently, the empirical semi-variogram is computed as follows:

$$\gamma(h) = \frac{1}{2n(h)} \sum_{i=1}^{n(h)} \left(z(x_i) - z(x_i+h)\right)^2 \tag{3}$$

where $z(x_i)$ and $z(x_i+h)$ are the binary pixel values (0 or 1) at distance x_i and x_i+h, respectively, and h is the lag in kilo-

meters. n represents the number of datapoints at a separation distance of h. The term $\gamma(h)$ is the semi-variance at separation distance h. Assuming that the empirical variogram is best represented by an exponential model, we fitted the functional parameters describing the spatial variability as follows:

$$\gamma(h) = c_0 + c(1 - e^{-h/C_L}) \tag{4}$$

where c_0 represents the nugget variance, c is the sill variance, and C_L is the distance parameter known as "correlation length." Conversely, the auto-correlation function is modeled as, $C = e^{-h/C_L}$, where "C" is the correlation. With the correlation length as an input, the Turning Bands algorithm then generates realizations of Gaussian random fields. The $N(0,1)$ spatially correlated random fields are then transformed to uniform $U[0,1]$ fields as follows:

$$x_j = \frac{1}{2} + \frac{1}{2}\mathrm{erf}(\varepsilon_j/\sqrt{2}) \tag{5}$$

where x_j, is a $U[0,1]$ random (but spatially correlated) deviate for pixel j generated from the corresponding $N(0,1)$ deviate, ε_j. The $\mathrm{erf}(\varepsilon_j)$ is the error function defined by the following integral:

$$\mathrm{erf}(\varepsilon_j) = \frac{2}{\sqrt{\pi}} \int_0^{\varepsilon_\mathrm{j}} \mathrm{e}^{-w^2} dw. \tag{6}$$

The uniform random field is then scaled by its standard deviation to yield a unitary variance (this ensures the maximum autocovariance of one at zero lag). Numerical consistency checks have shown that this conversion can increase the correlation length of the generated uniform distribution fields, which should be accounted for in setting the correlation length parameter for the generation of the Gaussian fields by the Turning Bands algorithm. It is noted, that the effect is most significant at lags beyond 10 (or 250 km range in this case). Hence, we ignored this suggested adjustment due to the relatively acceptable size ($\sim$ 250 km) of the study domain. Execution of step 2 yields spatially correlated fields of $U[0,1]$ random deviates that are now amenable for Bernoulli trials for modeling the uncertainty in rainy and nonrainy area delineation with consistent spatial structures. The estimation of correlation lengths for detection is further discussed in Section III (calibration).

C. Step 3: Modeling the Conditional Rain Rate Estimation Error

The conditional (reference rainfall>0 unit) satellite rain rates R_{SAT} are statistically related to corresponding conditional *reference rain rates* $R_{\mathrm{REF-INST}}$ as

$$R_{\mathrm{SAT}} = R_{\mathrm{REF-INST}} . \varepsilon_S \tag{7}$$

where the multiplicative satellite error parameter, ε_s, is assumed to be log-normally distributed. The assumption of log-normality was justified by the distinct skewness of the probability density function of error that was observed during the calibration exercise (discussed next). A log transformation $[\log(R_{\mathrm{SAT}}) - \log(R_{\mathrm{REF-INST}})]$ of (7) transforms the ε_s to a Gaussian $N(\mu, \sigma)$ deviate ε where μ and σ are the mean and standard deviation statistics, respectively. To determine the multiplicative mean (Mu_{INST}) and standard deviation (S_{INST}) of ε_s the following conversion is used in terms of μ and σ:

$$Mu_{\mathrm{INST}} = \exp(\mu + 0.5\sigma^2) \tag{8}$$

$$S^2_{\mathrm{INST}} = [\exp(\sigma^2) - 1]\exp(2\mu + \sigma^2). \tag{9}$$

The error parameter ε (hereafter, also referred to as "log-error") is both spatially and temporally auto-correlated. A lag-one autoregressive function is used as in [15] to model the temporal variability of μ (i.e., satellite rainfall bias)

$$\mu_{i,r} = \overline{\mu} + (\rho)(\mu_{i-1,r} - \overline{\mu}) \tag{10}$$

where time index i represents discrete hourly time-step, and ρ^2 is the lag-one autocorrelation of μ. Note that we use a subscript r to denote the index of a Monte Carlo (MC) realization. Herein, $\overline{\mu}$ represents the steady-state value of satellite bias. The variance of error $(\sigma^2_{i,r})$ at each time-step is related to the steady-state variance $(\overline{\sigma^2})$ and the lag-one correlation ρ^2 as

$$\sigma^2_{i,r} = \overline{\sigma^2}\left(1 - \left(\rho^2\right)\right). \tag{11}$$

The generation of spatial random fields of error with time-correlated mean (bias) is achieved as follows. At the first time-step, we set μ and σ to their corresponding steady state (ergodic) values that can be derived from a calibration exercise (discussed next), and generate a random field of errors. At subsequent time-steps i for a given MC realization, r, $\mu_{i,r}$ is calculated on the basis of (10) using the value from the previous time-step $i-1$. Note that for the previous time-step $i-1$ the $\mu_{i-1,r}$ is the sample value calculated on the basis of what is actually generated by a given random MC realization index r and, hence, will not equal the steady-state (population) value of $\overline{\mu}$ (unless the areal domain is infinitely large).

D. Generation of Synthetic Satellite Rainfall Fields With SREM2D

The *SREM2D* operation is summarized in the flow chart of Fig. 2. If the time-scale of reference rainfall is coarser than the time-scale of the satellite rainfall product, we use (1) and (2) to generate realizations of instantaneous reference rain rate values $(R_{\mathrm{REF-INST}})$. Pixels that are zero (nonrainy) do not require such treatment. Next, a Bernoulli trial is conducted for each satellite pixel to model the $\mathrm{POD}_{\mathrm{INST}}$ by generating a uniform $U[0,1]$ random number r_n. If r_n is less than $\mathrm{POD}_{\mathrm{INST}}$ (which is determined as a function of $R_{\mathrm{REF-ACCU}}$) an instantaneous reference rain rate, $R_{\mathrm{REF-INST}}$ value is calculated on the basis of (2) by randomly generating a log-normally distributed deviate, $LN[Mu_{\mathrm{INST-ACCU}}, S_{\mathrm{INST-ACCU}}]$, representing $E_{\mathrm{INST-ACCU}}$. After the conversion of an accumulated rain rate field to an instantaneous "reference" rain rate field, two sets of spatially correlated $U[0,1]$ random fields are generated, one each for conducting Bernoulli trials to model the satellite's successful delineation of rainy and nonrainy areas. This is done using (3)–(6) and the procedure described in step 2. When the instantaneous reference rain rate is nonzero $(R_{\mathrm{REF-INST}}>0)$ *SREM2D* decides as to whether the corresponding satellite rainfall estimate would be zero, or not, through a Bernoulli

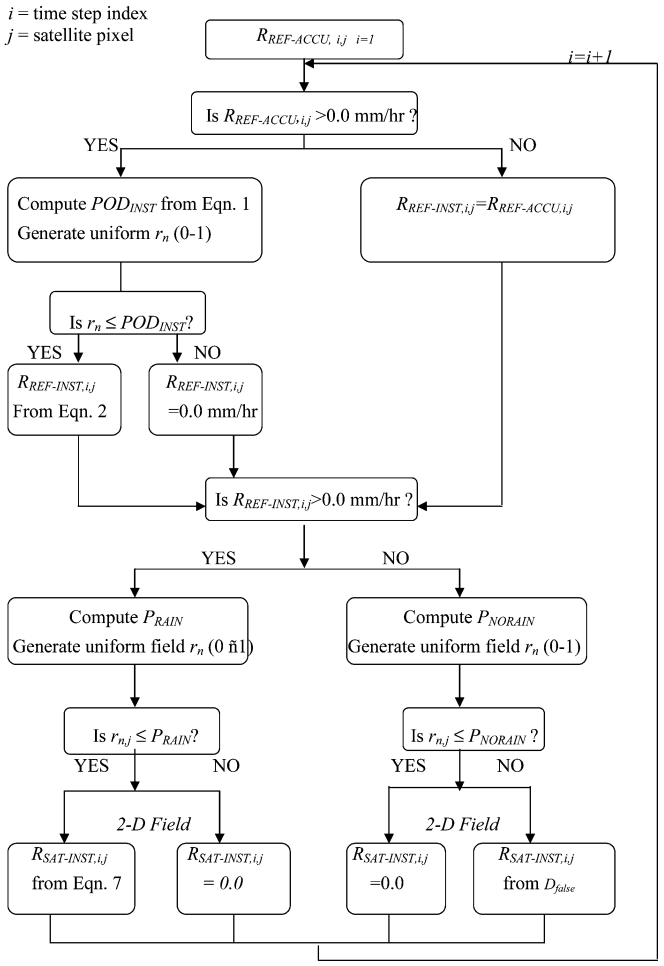

Fig. 2. Flowchart for *SREM2D* algorithm; i and j represent time-step and satellite pixel indexes.

trial. If the corresponding uniform $U[0,1]$ random number (obtained from the random field) r_n is less than P_{RAIN} (which is determined as function of $R_{\mathrm{REF-INST}}$) then the instantaneous satellite retrieval R_{SAT} is set a nonzero value determined stochastically from (7) (discussed next). Otherwise, R_{SAT} is assigned zero value. Similarly, for a nonrainy reference value ($R_{\mathrm{REF-INST}} = 0.0$ unit) Bernoulli trial is used to decide as to whether the satellite rainfall estimate would be zero or nonzero. If the uniform random deviate r_n generated for a given pixel is less than P_{NORAIN}, then R_{SAT} is assigned a zero value. Otherwise, the satellite rain rate value is statistically determined on the basis of the false alarm (i.e., false rain detection) satellite rain rates' probability density function (D_{false}). Having defined the pixels delineated as rainy, satellite rain rate values are stochastically simulated on the basis of space-time correlated error fields generated using (7)–(11) and the sequence enumerated in step 3. The procedure may be repeated multiple times to generate equiprobable ensembles of synthetic satellite retrieval fields.

III. SREM2D Calibration

Having mathematically formulated the algorithm for *SREM2D*, the next step is to calibrate the model parameters based on actual sensor retrievals. To demonstrate the algorithm

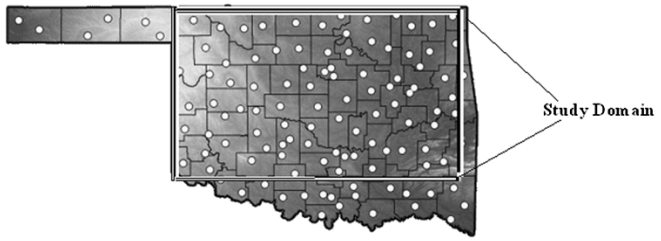

Fig. 3. Study region in the Southern plains bounded between $-100°$ W—95° W and 37° N–34° N. At 0.25–deg resolution, the domain comprises 20×12 pixels. The dots show the location of the Oklahoma Meso-network's meteorological stations.

in this study, we chose hourly IR rainfall product as the satellite rainfall source, and corresponding hourly ground radar rainfall fields as the reference input for *SREM2D*. In terms of the IR retrievals, we chose the NASA data product operationally known as IR-3B41RT (for a brief description see Section II, step 2). The data resolution was 0.25 deg and hourly. Radar rainfall fields were retrieved from WSR-88D observations using the National Weather Service multicomponent precipitation estimation algorithm with real-time adjustments based on mean-field radar-rain gauge hourly accumulation comparisons [9], [34], [33]. To minimize effects due to complex terrain and range effects the calibration exercise was performed over the region of Oklahoma bounded by $-100°$ W–95° W and 37° N $-34°$ N (Fig. 3). We selected a period of 4 months (May 1, 2002–August 31, 2002; 2952 hourly time-steps each with 20×12 pixels at 0.25 deg resolution) to determine the *SREM2D* error parameters. Step 1 of *SREM2D* algorithm did not apply in this application as both reference and satellite estimates had the same temporal resolution. About 3% of the IR data were missing from the archive, and replaced by radar data. We determined the values and/or functional forms of the following *SREM2D* error parameters: 1) P_{RAIN} (as a function of reference rainfall); 2) P_{NORAIN}; 3) D_{false}; 4) Mu_{INST} (8); 5) S_{INST} (9); 6) Correlation lengths for the successful delineation of rain—$\mathrm{CL}_{\mathrm{RAIN}}$; and 7) no rain—$\mathrm{CL}_{\mathrm{NORAIN}}$; (8) correlation length for the retrieval error (conditional, when rain >0.0 unit)—$\mathrm{CL}_{\mathrm{RET}}$; and (9) the lag-one hourly autocorrelation, ρ, of satellite bias.

Table I summarizes the fine-scale multidimensional error structure of IR-3B41RT. We computed the multiplicative bias (8) of the conditional retrieval by normalizing the total rainfall volume estimated by the sensor over the entire study period to that estimated by radar. Since the retrieval is conditional, only pixels that are successfully delineated as rainy by the sensor are considered. Due to the long time series, this yielded a climatologic estimate of satellite bias representative of the steady-state bias value for the region. About 125% overestimation of rainfall volume (multiplicative bias, $\mathrm{MU}_{\mathrm{INST}} = 2.25$) is observed with a log-error standard deviation of 1.27. Consistently with previous observations by Hossain and Anagnostou [15], the probability distribution of rainfall during false alarms appeared to follow an exponential density function with mean $(1/\lambda)$ equal to 1.43 mm/hr. The functional form of P_{RAIN} was found to follow a sigmoidal function (Fig. 4, right panel) with parameters A and B shown in Table I. Large spatial structures

TABLE I
SREM2D PARAMETERS EVALUATED FOR IR-3B41RT DATA AT 0.25- AND 0.5-deg RESOLUTION

Satellite Data	**IR-3B41RT**	
Scale (degree)	**0.25°**	**0.50°**
Multiplicative Bias	2.25	2.35
Gaussian Std. Deviation	1.27	2.53
False Alarm mean ($\frac{1}{\lambda}$) [1]	1.43 mm/hr	0.95 mm/hr
POD parameters A(B) [2]	1.1(1.5)	1.05(2.0)
POD_{NORAIN} (%)	95.60	94.60
Retrieval Error[4] Correlation Length (Spatial) [3]	170.0 km	250.0 km
Successful No-rain Detection Correlation Length[3] (Spatial)	220.0 km	220.0 km
Successful Rain Detection Correlation Length[3] (Spatial)	170.0 km	180.0 km
Lag-one (hourly) Correlation of retrieval error [4] (ρ) (temporal)	0.62	0.72

[1] $D_{false}(R_{SAT})=\lambda\exp(-\lambda R_{SAT})$ [Exponential distribution assumed on the basis of [15]]

[2] $\mathrm{POD}(R_{WSR\text{-}88D})=\dfrac{1}{A+\exp(-BR_{WSR-88D})}$ [Sigmoidal function assumed on the basis of [15]]

[3] An exponential autocorrelation model is assumed: $C = \mathrm{EXP}(-h/C_L)$ where C=correlation; h= distance or time and C_L= length or time at which C = 0.368

[4] Retrieval errors is defined as conditional (when WSR-88D rain rate>0.0 mm/hr)

with correlation lengths in excess of 150 km for the detection of rain, no-rain and retrieval error were observed (Table I and Fig. 5).

IV. SREM2D EVALUATION

A. Numerical Accuracy

Fig. 6(a) shows a typical *SREM2D*-simulated satellite rainfall field from May 13th, 00:00 hours (UT) (rightmost panel) and comparisons against the reference input (WSR-88D, leftmost panel) and true IR (3B41RT, middle panel). *SREM2D* appears to preserve the qualitative sanity of the rain fields by mimicking the observed IR spatial pattern. In Fig. 6(b), we observe that the rainy and nonrainy area delineation by *SREM2D* is quite similar in structure to that observed from sensor data. As part of a numerical consistency check, Table II shows the convergence of the simulated error statistics of *SREM2D* as a function of MC runs for 0.25-deg hourly resolution calibrated parameters. Due to the long time series (2952 time-steps) the ergodic hypothesis appears reasonably dominant here; 15 *SREM2D* MC realizations are found adequate to converge to the true statistics of the error structure. Fig. 7 shows the convergence pattern for a time series one order smaller (295 time-steps) than the entire 4-month study period. Here, convergence to the true error statistics (only multiplicative bias of retrieval is shown) is found to require an order higher number of MC runs ($\sim$100 runs). It is evident from Figs. 6 and 7 that for reasonably large ($>10 \times 10$ pixels) fields and sufficiently long ($>$1000 time-steps) time series, a parsimonious number of MC realizations in the range of 10–20 are adequate to statistically characterize the sensor's error structure, and provide sufficient ensemble representations

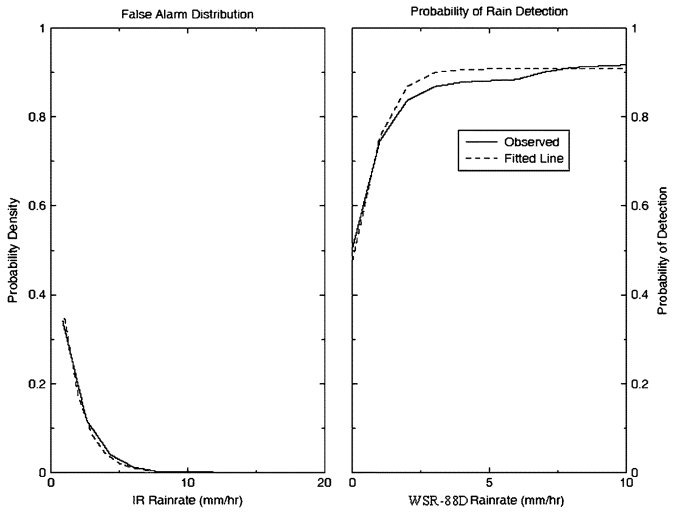

Fig. 4. Observed and fitted patterns of false alarm distribution and rain detection (POD) for IR-3B41RT at 0.25-deg resolution.

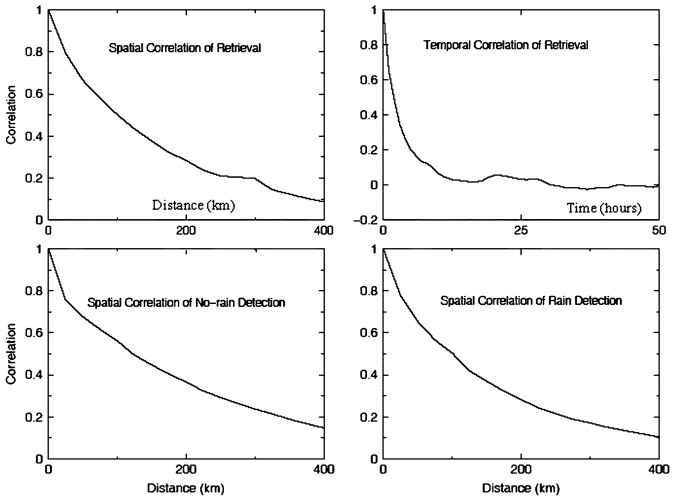

Fig. 5. Spatiotemporal behavior of IR-3B41RT error at 0.25-deg/hourly resolution. Upper left panel—spatial structure of retrieval error (conditional); upper right panel—temporal structure of retrieval error (conditional); lower left panel—spatial structure of successful no-rain detection; lower right panel—spatial structure of successful rain detection.

of error propagation in hydrological applications. For study periods comprising shorter scales (in space and time), it is important to ensure adequate MC runs according to some scaling rule of thumb based on actual testing of convergence of the *SREM2D* error parameters.

B. Scaling Consistency

The scale consistency of *SREM2D* is assessed using aggregated rainfall fields at coarser resolution (0.5 deg). The approach is to simulate ensembles (all 15 simulation runs of Table II) of *SREM2D* rainfall fields from WSR-88D reference rain fields at 0.25-deg resolution, and aggregate them to derive error parameters (of Table I) at 0.5-deg resolution. To assess the model's scaling consistency, the error parameters evaluated at coarse (0.5 deg) resolution are compared to corresponding error parameters calculated on the basis of comparisons of aggregated (true) IR-3B41RT versus WSR-88D data at the same resolution. To facilitate the comparison we define a scaling coefficient as

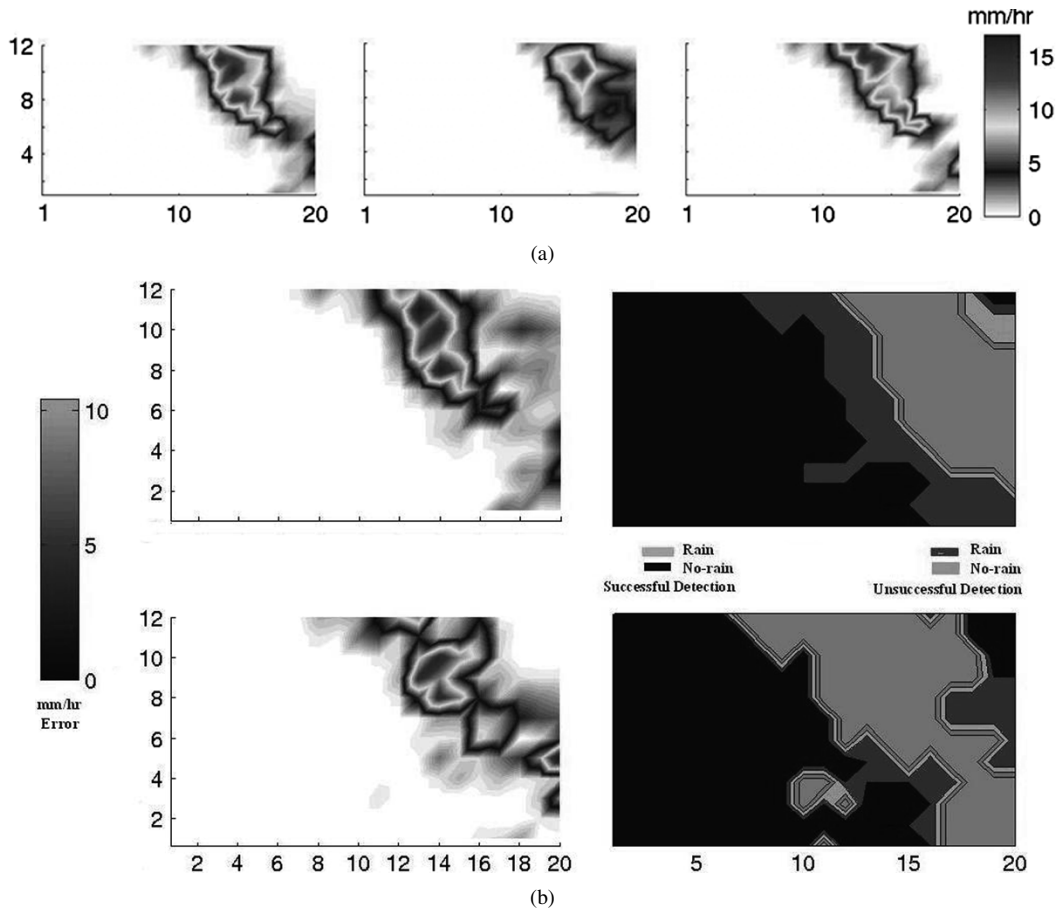

Fig. 6. (a) Examples of *SREM2D* simulated fields (rightmost) versus WSR-88D (leftmost) and actual IR (3B41RT) (middle panel) for May 13th, 00:0 Hrs, 2002 (UTC). (b) Maps of the error in retrieval (absolute difference) (left panels) and rainy and nonrainy area delineation (right panels) for the May 13th, 000 Hrs (UT). Upper panels—IR-3B41RT; Lower panels—*SREM2D* simulation. Colors have the same significance as in Fig. 1.

the ratio of the error parameters at 0.25-deg to that of 0.5-deg resolution.

Table III shows comparisons of the scaling coefficient values of *SREM2D*-simulated and actual data (IR-3B41RT). Accurate error structure preservation is observed at higher scales for the spatiotemporal correlation lengths with negligible error ranging between 5% and 10%. *SREM2D* yields an increase in standard deviation of log-error at the 0.5-deg scale due to the aggregation of false alarms and rain detection failures, which is also supported by the actual IR-3B41RT data. In Figs. 8–10, we show graphical representation of certain error properties for *SREM2D* and IR-3B41RT data. The false alarm and rain detection probability distributions shown in Fig. 8 (left and right panels) exhibit reasonable agreement between *SREM2D* and actual data. We note that the probability of rain detection at the aggregated resolution by *SREM2D* continues to preserve the idealized sigmoidal form and is mimicking well actual data at rain rates higher than 5 mm/hr. In Fig. 9, the spatiotemporal error structure of the aggregated *SREM2D* rain fields agree well with that obtained from aggregation of IR-3B41RT retrievals. The left panel denotes the spatial correlogram. The temporal dynamics of estimation bias (i.e., the temporal corelogram of μ) is accurately preserved, even at high lags ($>$200 h) where white noise is expected to dominate (Fig. 9, right panel). Finally, in Fig. 10, we show comparisons for the corelograms of successful delineation for rainy and nonrainy areas.

For a quantitative assessment of the statistical significance of the scaling consistency, Table IV shows the *chi-square* statistic computed from deviations observed between *SREM2D* and IR-3B41RT data in Figs. 8–10. Herein, we test the null hypothesis that *SREM2D* simulations shown in those figures are statistically similar to those of IR-3B41RT at the 5% confidence level. We define *chi-square* χ^2 as follows:

$$\chi^2 = \sum_{i=1}^{df} \frac{(x_{\mathrm{SREM2D}}i - x_{3B41\mathrm{RT}}i)^2}{x_{3B41\mathrm{RT}}i} \tag{12}$$

where *df* symbolizes the degree of freedom and subscripts refer to parameter values for the ith degree of freedom. The *df* represents the number of data points used to construct the scaling behavior in Figs. 8–10, and x represents the ordinate values. We show in Table IV through the *chi-squared* test that there is sufficient statistical evidence not to reject the null hypothesis at 5% confidence [22].

C. Comparison With Simpler Error Modeling Approaches

In this section, we compare the scaling consistency of our proposed model with two simpler error-modeling approaches. Both of these approaches assume the satellite retrieval to be perfect in terms of delineation of rainy and nonrainy areas, and having low, or none (one of the two), spatial and temporal error

TABLE II
NUMERICAL VERIFICATION OF SREM2D (time series = 2952 TIME-STEPS)

Total Number of Simulation Runs	P_{RAIN} @ $Rain_{WSR-88D}$ =2.5mm/hr	P_{NORAIN}	Bias Multiplicative	Std. Dev Gaussian	Lag-1 Temporal Correlation ρ	False Alarm Mean (1/λ) mm/hr
Model Input[1]	**0.890**	**0.956**	**2.20**	**1.27**	**0.620**	**1.430**
1	0.898	0.951	4.10	1.68	0.640	1.415
2	0.896	0.951	2.16	1.24	0.611	1.423
3	0.894	0.953	1.89	1.13	0.640	1.427
4	0.892	0.952	2.10	1.22	0.628	1.428
5	0.895	0.952	2.03	1.19	0.629	1.427
6	0.896	0.952	2.10	1.22	0.626	1.427
7	0.897	0.952	2.01	1.21	0.636	1.424
8	0.898	0.952	2.01	1.23	0.631	1.424
9	0.897	0.952	1.92	1.23	0.625	1.424
10	0.897	0.952	1.93	1.24	0.625	1.425
11	0.898	0.952	1.93	1.24	0.625	1.425
12	0.898	0.952	1.96	1.24	0.625	1.425
13	0.898	0.952	1.96	1.24	0.625	1.425
14	0.898	0.952	1.95	1.24	0.625	1.425
15	***0.898***	***0.952***	***1.95***	***1.24***	***0.625***	***1.425***

1. *Model Input* is the input parameters to *SREM2D* at 0.25 degree (Table 1).

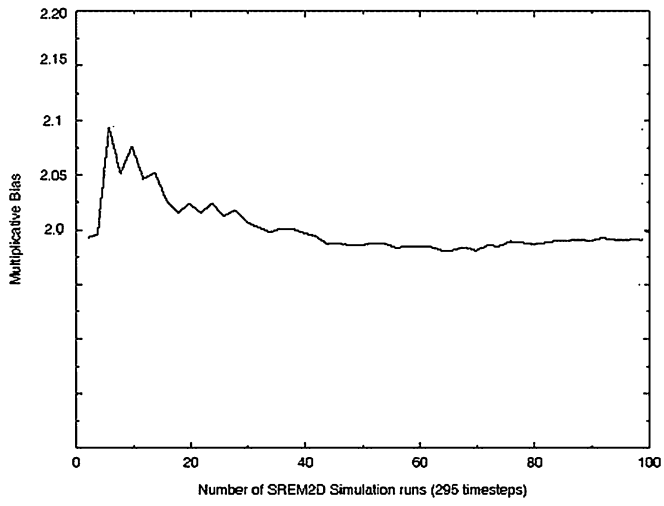

Fig. 7. Convergence of *SREM2D* multiplicative bias for 295 time-step time series (data period 1 order smaller than that shown in Table II). One hundred simulations appear adequate for convergence to the required error parameter (in this case, multiplicative bias), which, for Table II is found to be 15 simulation runs.

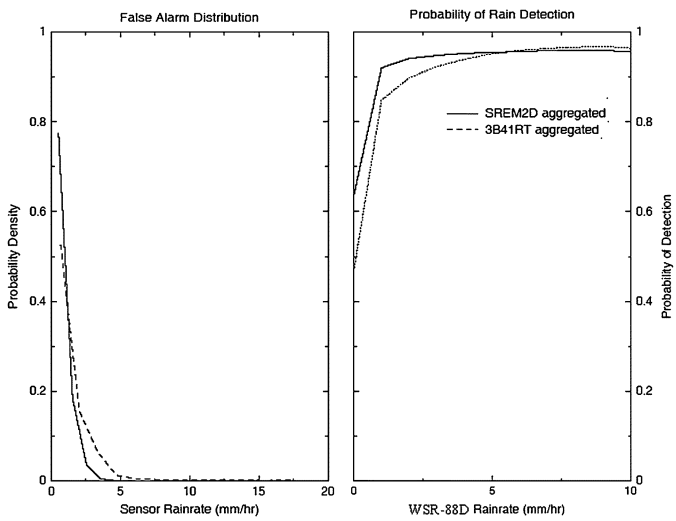

Fig. 8. Comparison of the scaling behavior of *SREM2D* simulations with real IR-3B41RT data for false alarms and successful detection of rain at 0.5-deg resolution.

structure. We name the two simpler approaches to error modeling as $N1$ and $N2$. In approach $N1$, we model only the conditional retrieval error (assuming perfect detection) with no spatiotemporal error structure. The systematic (mean) and random

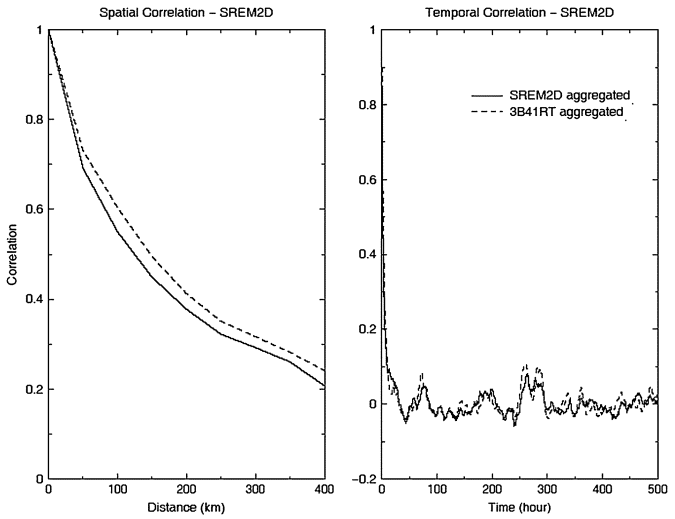

Fig. 9. Comparison of scaling behavior of *SREM2D* simulations with 3B41RT for spatiotemporal structure of rain retrieval error (conditional) at 0.50 deg resolution. Left panel—spatial correlogram for random error; Right panel—temporal correlogram for retrieval bias.

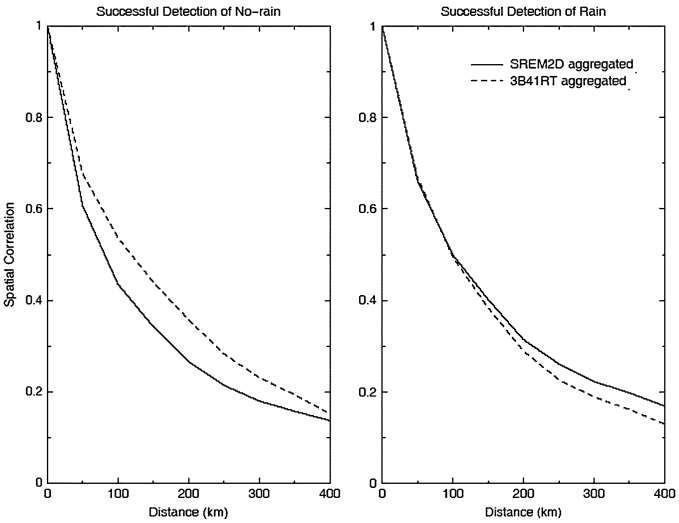

Fig. 10. The spatial correlograms for successful delineation of nonrainy areas (left panel) and rainy areas (right panel).

(variance) error parameters chosen for this purpose are those shown in Table I. Approach $N2$ also assumes perfect detection, but models the conditional retrieval error with the herein specified spatiotemporal structural parameters as listed in Table I (notably: $\mathrm{CL}_{\mathrm{RET}}$, and lag-one correlation, ρ). These two simpler approaches are bi-dimensional in the sense that they recognize only the systematic and random error components as the major constituents of the error structure. They ($N1$ and $N2$) continue to be the backbone of recent hydrologic error propagation studies [29], [38]. Fig. 11 shows a rain field realization simulated by the two approaches for May 13, 00:00 hours, 2002 [similar to Fig. 6(a) by *SREM2D*]. We summarize the scaling coefficients for the $N1$ and $N2$ methods in Table IV. While we observe that the scaling coefficients for the retrieval correlation length and lag-one hourly correlation are preserved within acceptable bounds relative to IR-3B41RT data for the approach $N2$, poor preservation of the structure for random error (standard deviation) is observed at the higher scale of aggregation.

TABLE III
SUMMARY OF SCALING BEHAVIOR OF IR-3B41RT AND SREM2D

	IR-3B41RT		***SREM2D***	
Scale (degree)	**0.25 / 0.5**	**Scaling Coeff.**[1]	**0.25 / 0.5**	**Scaling Coeff.**[1]
Multiplicative Bias	2.25/2.35	**0.96**	1.95/2.00	**0.97**
Std. Dev (Gaussian)	1.27/ 2.53	***0.50***	1.24/1.99	***0.62***
False Alarm mean (mm/hr)	1.428 / 0.950	***1.50***	1.425 / 0.750	***1.90***
Retrieval Error Correlation Length (spatial - km)	170.0 / 250.0	***0.68***	160.0 / 240.0	***0.67***
Lag-one hourly correlation (temporal)	0.620/ 0.720	***0.86***	0.619 / 0.702	***0.88***

1. Scaling Coefficient = Ratio of error statistic at 0.25 degree-hourly to 0.5 degree-hourly.

We note more than 100% underestimation of the standard deviation of simulated retrieval error compared to IR-3B41RT derived error for both approaches ($N1$ and $N2$). When compared to *SREM2D* (which is below 30%), we observe that the underestimation of the random error variability is significant. In the aggregation process, the two simpler approaches fail to mimic the increase in the standard deviation of random error apparent in the actual sensor data (Table IV). This underestimation denotes the importance of modeling probabilistically the satellite error characteristics in delineating rainy from nonrainy areas. The assessment of hydrologic implications of satellite rainfall error by those simpler error-modeling approaches (such as $N1$ or $N2$) may deviate even further in error propagation of hydrologic simulations given the nonlinear nature of the land-atmosphere interaction processes at fine space-time scales. Earlier studies by Anagnostou [3] have shown that rain retrieval differences can significantly magnify in the prediction of land surface parameters (soil moisture, runoff, energy fluxes, etc.). Similarly, Hossain and Anagnostou [15] have demonstrated significant sensitivity on the estimation of the water budget and peak runoff in terms of the sensor's rain area delineation accuracy, especially in the case of long lasting storm events ($>$3 days).

V. CONCLUSION

SREM2D was developed for generating ensembles of realistic satellite rainfall fields. This space-time error model utilizes higher accuracy "reference" rain fields to characterize the multidimensional stochastic error structure of satellite retrieval as a function of scale. Comparison with actual sensor data revealed that *SREM2D* is capable of preserving the satellite retrieval error characteristics across two scales (0.25–0.5 deg) with less than 30% underestimation when compared to actual data. Two simpler, but widely used, approaches of error modeling with no explicit formalization of the delineation error of rainy/nonrainy

TABLE IV
Chi-squared STATISTIC OF THE SCALING BEHAVIOR OF *SREM2D* SIMULATIONS USING IR-3B41RT AS REFERENCE (TRUTH)

	Chi-squared Statistic					
	False Alarm Distribution (Figure 8, left panel)	Probability of Rain Detection (Figure 8, right panel)	Temporal correlogram for bias (Figure 9, right panel)	Spatial Correlogram of rain rate error (Fig. 9, left panel)	Spatial Correlogram of non-rain detection error (Fig. 10, left panel)	Spatial Correlogram of rain detection error (Fig. 10, right panel)
Degrees of Freedom, *df*	10	10	10	10	10	10
χ^2	0.1540	0.0689	0.1446	0.0249	0.1083	0.0347
Significance at 5% level	Yes	Yes	Yes	Yes	Yes	Yes

$\chi^2 = \sum_{i=1}^{df} \frac{(x_{SREM2D}i - x_{3B41RT}i)^2}{x_{3B41RT}i}$, where *df* = degree of freedom and subscripts refer to parameter values for i^{th} degree of freedom

TABLE V
SCALING CONSISTENCY OF THE SIMPLER ERROR MODELS ($N1$ AND $N2$)

	IR-3B41RT		Simpler Error Model			
			Without Spatio-temporal structure (*N1*)		With Spatio-temporal structure (*N2*)	
Scale (degree)	0.25/0.50	Scale Coeff.	0.25/0.50	Scale Coeff.	0.25/0.50	Scale Coeff.
Multiplicative Bias	2.25/2.35	**0.96**	1.83/1.87	**0.98**	1.83/1.87	**0.98**
Std. Dev. (Gaussian)	1.27/2.53	***0.50***	1.27/1.53	***0.83***	1.27/1.53	***0.83***
Retrieval Error Correlation Length (spatial – km)	170/250	***0.68***	N/A	N/A	160.0/220	***0.73***
Lag-one hourly correlation (temporal)	0.62/0.72	***0.86***	N/A	N/A	0.619/0.740	***0.83***

areas revealed that preservation of the retrieval error structure across scale is not honored. Large underestimation exceeding 100% in the random retrieval error was observed.

Our proposed stochastic modeling strategy offers a more comprehensive and explicit characterization of satellite error in space and time. Furthermore, the decomposition of error

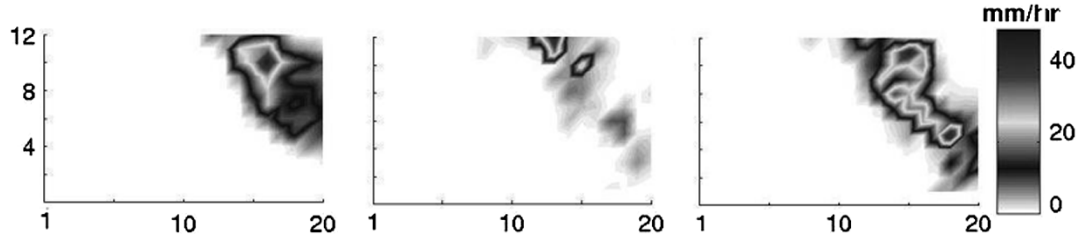

Fig. 11. Comparison of rain fields generated by two simpler approaches. Left most panel—true IR-3B41RT; middle panel—approach N1 (no spatiotemporal structure); right panel—approach N2 (spatiotemporal structure).

structure into nine parameters (or dimensions) also allows a more complete exploration of the response surface of the hydrological error propagation (such as error in runoff or soil moisture simulation) within the satellite rainfall error hyperspace. An added versatility of *SREM2D* is that it is independent of the rain retrieval algorithm; thus, it can consistently apply to characterize the error structure of any satellite retrieval or combination of sensor estimates. This provides an objective way to compare competing rain estimation schemes by providing a quantitative assessment of hydrologic propagation error [15].

An important issue to note about SREM2D is that of regional dependency of its parameters, and consequently, of the model global applicability. Parameters controlling the spatial structure of error in SREM2D may be regionally calibrated using coincident TRMM-PR rainfall data (Hossain and Anagnostou 2004). However, the temporal error parameters require calibration with continuous reference rainfall data, which may be available from ground observations. Unfortunately, no rigorous global validation of current satellite rain retrievals (such as the TRMM precipitation products) has been performed, and it is not known yet as to whether the existing validation sites are sufficient, or good enough, to provide global validation of precipitation products in general. However, there has been significant work on globally classifying rain systems and finding similarities and differences between rain systems from various geographic regions [11], [31]. Potentially, such work could be used to identify the model error parameters, based on similarity with other regions, for the regions where validation sites are not available.

Two studies by Hossain and Anagnostou ([15] and [16]) have shown evidence that concepts formalized in *SREM2D* can effectively advance our understanding on the use of high-resolution satellite data in hydrologic applications. With the detailed space-time formulation of *SREM2D*, we hope that several questions on the hydrologic implications of satellite rainfall data can now be investigated on the basis of MC data driven experiments. Examples are: *What is the current level of performance of satellite rainfall data for surface hydrologic applications? At what level would a combined rainfall product need to perform in order to be more reliable than what it is today? What are the hydrologic variables that magnify or dampen in response to satellite rainfall error propagation? What are the tradeoff relationships between hydrologic simulation accuracy and satellite rainfall as space-time scales are increased or decreased?* The error model developed in this paper would facilitate the incorporation of a wide range of hydrologic model structures, resolutions and objectives toward optimal integration of remotely sensed rainfall data in data assimilation systems such as *GLDAS* for weather forecasting, and the upcoming GPM for flood forecasting over ungauged basins.

Finally, in addition to the science questions highlighted above, *SREM2D* may potentially have some applicability over ungauged regions in operational (online) frameworks currently serving society. Given that meteorological satellites on geostationary platforms have evolved over the years with the capability to provide high-frequency IR rainfall estimates over the vast un-gauged regions, an application of *SREM2D* wherein the definition of reference rainfall input and sensor estimate output is reversed should, in principle, yield equiprobable realizations of surface-based or ground reference measurements. Combined with the recently reported technique of C-MORPH [21], where information from the more accurate PM sensors are propagated by motion vectors derived from IR data, the inverse-*SREM2D* method of stochastic recreation of "reference rainfall" may provide hydrologically useful information in LSM. In addition, techniques of spatiotemporal disaggregation proposed by Venugopal [37] and Margulis and Entekhabi [27] could be embedded, in *SREM2D* algorithm to study the error propagation of coarser satellite rainfall datasets such as the Global Precipitation Climatology Project (GCPC) [18]. We caution the reader that our proposed inverse-*SREM2D* concept combined with suggested statistical downscaling techniques requires thorough verification before we can rightly proclaim its qualification in operational applications over un-gauged regions. Such a thorough assessment is underway and we hope to report findings in near future.

ACKNOWLEDGMENT

The authors would like to thank the three anonymous reviewers for their insightful comments.

REFERENCES

[1] P. A. Arkin and B. N. Meisner, "The relationship between large-scale convective rainfall and cold cloud cover western hemisphere during 1982–1984," *Monthly Weather Rev.*, vol. 115, pp. 51–74, 1987.

[2] I. Astin, "A survey of studies into errors in large scale space-time averages of rainfall, cloud cover, sea surface processes and the earth's radiation budget as derived from low orbit satellite instruments because of their incomplete temporal and spatial coverage," *Surveys Geophys.*, vol. 18, pp. 385–403, 1997.

[3] E. N. Anagnostou, "Assessment of satellite rain retrieval error propagation in the prediction of land surface hydrologic variables," in *Measuring Precipitation from Space: EURAINSAT and the Future*, V. Levizzani, P. Bauer, and F. J. Turk, Eds. Norwell, MA: Kluwer, 2005.

[4] E. N. Anagnostou and C. Morales, "Rainfall estimation from TOGA radar observations during LBA field campaign," *J. Geophys. Res.-Atmos.*, vol. 107, no. D18, pp. 35-1–35-14, 2002.

[5] E. A. Smith, G. Asrar, Y. Furuhama, A. Ginati, C. Kummerow, V. Levizzani, A. Mugnai, K. Nakamura, R. Adler, A. Mugnai, V. Casse, M. Cleave, M. Debois, J. Durning, J. Entin, P. Houser, T. Iguchi, R. Kakar, J. Kaye, M. Kojima, D. Lettenmaier, M. Luther, A. Mehta, P. Morel, T. Nakazawa, S. Neeck, K. Okamoto, R. Oki, G. Raju, M. Shepherd, E. Stocker, J. Testud, and E. Wood, "The international global precipitation measurment (GPM) program and mission: An overview," in *Measuring Precipitation from Space: EURAINSAT and the Future*, V. Levizzani and F. J. Turk, Eds. Norwell, MA: Kluwer, 2005.

[6] M. X. Chen, X. B. Zeng, and R. E. Dickinson, "Adjustment of GCM precipitation intensity over the United States," *J. Appl. Meteorol.*, vol. 37, pp. 876–887, 1998.
[7] T. Chronis, E. N. Anagnostou, and T. Dinku, "High-frequency estimation of thunderstorms via satellite infrared and a long-range lightning network in Europe," *Quart. J. Roy. Meteorol. Soc. B.*, vol. 130, no. 599, pp. 1555–1575, 2004.
[8] Y. Dai, X. Zeng, R. E. Dickinson, I. Baker, G. B. Bonan, M. G. Bosilovich, S. Denning, P. Dirmeyer, P. R. Houser, G. Niu, K. W. Oleson, A. Schlosser, and Z.-L. Yang, "The common land model," *Bulletin Amer. Meteorol. Society (BAMS)*, pp. 1013–1023, Aug. 2003.
[9] R. A. Fulton, J. P. Breidenbach, D.-J. Seo, D. A. Miller, and T. O'Bannon, "The WSR-88D rainfall algorithm," *Weather Forecast.*, vol. 13, no. 2, pp. 377–395, 1998.
[10] M. Gebremichael and W. Krajewski, "Characterization of temporal sampling error in space-time-averaged rainfall estimates from satellites," *J. Geophys. Res.—Atmospheres*, vol. 109, no. D11, 2004.
[11] B. Geerts and T. Dejene, "Regional and diurnal variability of the vertical structure of precipitation systems in Africa based on spaceborne radar data," *J. Climate*, vol. 18, pp. 893–916, 2005.
[12] M. A. Giordano and A. T. Wolf, "Sharing waters: Post-Rio international water management," *Natural Resources Forum*, vol. 27, pp. 163–171, 2003.
[13] G. C. Griffith, W. L. Woodley, and P. G. Grube, "Rain estimation from geosynchronous satellite imagery-visible and infrared studies," *Monthly Weather Rev.*, vol. 106, pp. 1153–1171, 1978.
[14] F. Hossain, "Toward formulation of a fully space-borne early warning system for floods: Can cost-effectiveness outweigh prediction uncertainty?," *Natural Hazards*, vol. 37, no. 3, pp. 263–276, 2006.
[15] F. Hossain and E. N. Anagnostou, "Assessment of current passive microwave and infrared based satellite rainfall remote sensing for flood prediction," *J. Geophys. Res.-Atmos.*, vol. 109, 2004.
[16] F. Hossain and E. N. Anagnostou, "Numerical investigation of the impact of uncertainties in satellite rainfall and land surface parameters on simulation of soil moisture," *Adv. Water Resources*, vol. 28, no. 12, pp. 1336–1350, 2004.
[17] F. Hossain, E. N. Anagnostou, and T. Dinku, "Sensitivity analyzes of satellite rainfall retrieval and sampling error on flood prediction uncertainty," *IEEE Trans. Geosci. Remote Sens.*, vol. 42, no. 1, 2004.
[18] G. J. Huffman *et al.*, "Global precipitation at one-degree daily resolution from multisatellite observations," *J. Hydrometeorology*, vol. 2, pp. 36–50, 2001.
[19] G. J. Huffman, R. F. Adler, E. F. Stocker, E. J. Bolvin, and E. J. Nelkin, "Analysis of TRMM 3-hourly multisatellite precipitation estimates computed in both real and post-real time," presented at the *12th Conf. Satellite Meteorol. Oceanog.*, vol. 2, Long Beach, CA, Feb. 2003, Paper P4.11.
[20] J. E. Janowiak, R. J. Joyce, and Y. Yarosh, "A real-time global half-hourly pixel-resolution infrared dataset and its applications," *Bulletin Amer. Meteorol. Soc.*, vol. 82, no. 2, pp. 205–217, 2001.
[21] R. J. Joyce, J. E. Janowiak, P. A. Arkin, and P. Xie, "CMORPH: A method that produces global precipitation estimates from passive microwave and infrared data at high spatial and temporal resolution," *J. Hydrometeorology*, vol. 5, pp. 487–503, 2004.
[22] R. Johnson, *Miller and Freund's Probability and Statistics for Engineers*. Englewood Cliffs, NJ: Prentice-Hall, 2004, p. 302.
[23] C. Kummerow, Y. Hong, W. S. Olson, S. Yang, R. F. Adler, J. McCollum, R. Ferraro, G. Petty, D.-B. Shin, and T. T. Wilheit, "The status of the tropical rainfall measuring mission (TRMM) after two years in orbit," *J. Appl. Meteorol.*, vol. 39, no. 12, pp. 1965–1982, 2000.
[24] ——, "Evolution of the Goddard profiling algorithm (GPROF) for rainfall estimation from passive microwave sensors," *J. Appl. Meteorol.*, vol. 40, pp. 1801–1821, 2001.
[25] L. Liao, R. Meneghini, and T. Iguchi, "Comparisons of rain rate and reflectivity factor derived from the TRMM precipitation radar and the WSR-88D over the Melbourne, Florida site," *J. Atmosph. Oceanic Technol.*, vol. 18, pp. 1959–1974, 2001.
[26] A. Mantoglou and J. L. Wilson, "The turning bands method for simulation of random fields using line generation by a spectral method," *Water Resources Res.*, vol. 18, no. 5, pp. 1379–1394, 1982.
[27] S. Margulis and D. Entekhabi, "Temporal disaggregation of satellite-derived monthly precipitation estimates and resulting propagation of error in partitioning of water at the land surface," *Hydrol. Earth Syst. Sci.*, vol. 5, no. 1, pp. 27–38, 2001.
[28] A. J. Negri, R. F. Adler, and L. Xu, "A TRMM-calibrated rainfall algorithm applied over Brazil," *J. Geophys. Res.*, vol. 107, 2002.
[29] B. Nijssen and D. P. Lettenmaier, "Effect of precipitation sampling error on simulated hydrological fluxes and states: Anticipating the global precipitation measurement satellites," *J. Geophys. Res.*, vol. 109, 2004.
[30] G. N. Paudyal, "Forecasting and warning of water-related disaster in a complex hydraulic setting—The case of Bangladesh," *Hydrolog. Sci. J.l*, vol. 47(S), pp. S5–S18, 2002.
[31] W. A. Petersen and S. A. Rutledge, "Regional variability in tropical convection: Observations from TRMM.," *J. Climate*, vol. 14, pp. 3566–3586, 2002.
[32] M. Rodell, P. R. Houser, U. Jambor, J. Gottschalck, K. Mitchell, C.-J. Meng, K. Arsenault, B. Cosgrove, J. Radakovich, M. Bosilovich, J. K. Entin, J. P. Walker, D. Lohmann, and D. Toll, "The global land data assimilation system," *Bull. Amer. Meteorol. Soc.*, vol. 85, no. 3, pp. 381–394, 2004.
[33] D.-J. Seo *et al.*, "Real-time adjustment of range-dependent biases in WSR-88D rainfall estimates due to nonuniform vertical profile of reflectivity," *J. Hydrometeorology*, vol. 1, no. 3, pp. 222–240, 2000.
[34] D.-J. Seo, J. P. Breidenbach, and E. R. Johnson, "Real-time estimation of mean field bias in radar rainfall data," *J. Hydrology*, vol. 223, no. 3–4, pp. 131–147, 1999.
[35] T. H. Syed, V. Lakshmi, E. Paleologos, D. Lohmann, K. Mitchell, and J. Famiglietti, "Analysis of process controls in land surface hydrological cycle over the continental United States," *J. Geophys. Res.*, vol. 109, 2004.
[36] M. Steiner, T. L. Bell, Y. Zhang, and E. F. Wood, "Comparison of two methods for estimating the sampling-related uncertainty of satellite rainfall averages based on a large radar dataset," *J. Climate*, vol. 16, pp. 3759–3778, 2003.
[37] V. Venugopal, E. Foufoula-Georgio, and V. Sapozhinikhov, "A space-time downscaling model for rainfall," *J. Geophys. Res.-Atmos.*, vol. 104, no. D16, pp. 19 705–19 721, 1999.
[38] J. P. Walker and P. Houser, "Requirements of a global near-surface soil moisture satellite mission: Accuracy, repeat time, and spatial resolution," *Adv. Water Res.*, vol. 27, pp. 785–801, 2004.
[39] C. Morales and E. N. Anagnostou, "Extending the capabilities of high-frequency rainfall estimation from geostationary-based satellite infrared via a network of long-range lightning observations," *J. Hydrometerology*, vol. 4, no. 2, pp. 141–159, 2003.

Faisal Hossain received the B.S. degree from Banaras Hindu University, Varanasi, India, the M.S. degree from The National University of Singapore, Singapore, and the Ph.D. from The University of Connecticut, Storrs, in 1996, 1999, and 2004, respectively.

Prior to that, his research interests comprise a three-dimensional approach to water resources engineering for the water-stressed 21st century. These are: 1) improved land-surface applications of present and planned hydrologic remote sensing missions (space-borne and ground networks); 2) integration of conventional statistical theory with fuzzy concepts for cost-effective management of contaminated hydrosystems; and 3) development of computationally robust probabilistic schemes for improved hydrologic characterization of geosystems.

Emmanouil N. Anagnostou received the B.S degree from the National Technical University, Athens, Greece, in 1990 and the M.S. and Ph.D. degrees from The University of Iowa, Iowa City, in 1995 and 1997, respectively, all in civil and environmental engineering.

He is currently an Associate Professor in the Civil and Environmental Engineering Department, University of Connecticut, Storrs. His primary research focuses on developing techniques for remote sensing of precipitation parameters ranging from lightning detection to the retrieval of precipitation profiles and surface rainfall from satellite and ground-based sensors. Other research interests include the optimal integration of rainfall remote sensing products in hydrologic modeling systems for the prediction of floods and studying regional water and energy cycle.